Jan Heitmann, Fabian Steinmetz and Christian Renner. Self-Localization of Micro AUVs Using a Low-Power, Low-Cost Acoustic Modem. In Proceedings of the OCEANS Conference 2018, Charleston, SC, USA, Oct. 2018

Self-Localization of Micro AUVs Using a Low-Power, Low-Cost Acoustic Modem

Jan Heitmann, Fabian Steinmetz, Christian Renner
Research Group smartPORT
Hamburg University of Technology
Email: {jheitmann, fabian.steinmetz, christian.renner}@tuhh.de

Abstract—Sensing tasks underwater, i.e. monitoring water quality, spillage detection or pillar inspection, are becoming more and more important for port operators, researchers and local authorities. The accomplishment of these tasks is dangerous, costly and time consuming. A variety of cheap micro AUVs has been presented by industry and academia in the last years. However, to enable autonomous sensing tasks underwater, these devices have to be able to send their data to the surface and to be aware of their own position. The use of expensive hardware for that contradicts the implementation of cheap μAUVs. In this paper, we present a lightweight ranging and localization approach, solely relying on two-way ranging. We analyze the performance of our proposed approach during in a practical evaluation and show that self-localization solely relying our self-developed, small and inexpensive underwater acoustic modem, the μAUVs HippoCampus and a hydrophone is feasible.

I. Introduction

The sensing of underwater parameters as well as the inspection of objects below the water surface is needed in many different applications. In one of these cases quality of bathing water has to be monitored to ensure healthy conditions for the population. The detection of cyano is an important example for that. At a higher scale the measuring of water parameters e.g. temperature is required to observe submesoscale eddies in the oceans, as presented in [1]. The inspection of industrial inlets to enforce the adherence to environment protection laws is not less important. The inspection of objects in the water, such as sheet pillars or sunken ships, is another example for the need of underwater monitoring and sensing.

All the mentioned applications and use cases have in common that they are costly, complex and dangerous, because most of them are executed by divers, or a vessel. Currently, they all require human intervention. The implementation of inexpensive autonomous devices taking over theses tasks is therefore highly desirable.

However, most of these tasks are not stationary, making the usage of a static sensor network impracticable. Furthermore, fast reaction times and high spatial resolution are often needed, making the deployment of a single sensing device also pointless.

To fulfill these requirements, the usage of small and low-cost autonomous underwater vehicles (μAUVs) such as MONSUN [2], [3] or HippoCampus [4] is advisable. A length of less than 1 m allows deployment in narrow places and agile navigation. To obtain a large area of coverage, the deployment of these μAUVs in formations or swarms is desired. As multiple μAUVs are needed for formations or swarms, the single device should be low cost. The commonly restricted budget of the user (often local authorities) makes this even more important.

The ability to communicate with other swarm members is mandatory for the implementation of efficient swarm algorithms. Knowledge on the current position of these μAUVs is needed, to ensure retaining of the current formation and the ability to georeference measured parameters. Following the need for low-cost swarm members, the communication and localization has also be done with a low-cost device, or in the best case, without additional hardware.

A. Contributions

In this paper we analyze the feasibility of self-localization of μAUVs solely relying on small, low-cost acoustic underwater modems. The solution we evaluate requires a single acoustic receiver, capable of capturing time-of-flight of an acoustic signal and no other additional hardware, such as transceiver array, DVLs or else. The ranging we propose is piggy-backed on communication, needed anyway for transmitting status reports and sensor values. The presented localization algorithm is therefore bandwidth efficient, does not require fixed anchors or absolute time synchronization between nodes, and is non-centralized. The use case of the proposed solution are small, low-cost μAUVs, equipped with likewise low-cost acoustic modems.

In the following, we first describe our approach for distance-based ranging in general and the influence of speed-of-sound measuring based on that. Then, our simple, low-complex localization algorithm is presented in detail. Next, we describe the hardware used for evaluation. In the following we present a practical evaluation of a) our ranging approach, b) the localization in the static case and c) the localization in the mobile case. We practically analyze how well self-localization relying on cheap hardware is feasible and describe the problems we faced during our evaluation. Before we conclude the paper with a summary and future work, we present related

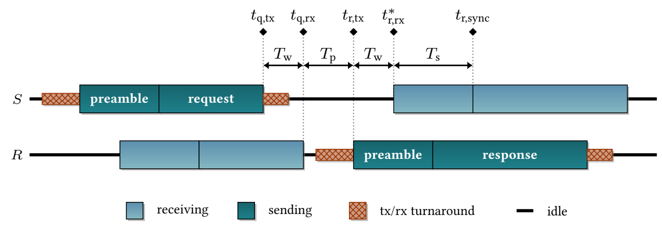

Fig. 1: Two-way time-of-flight ranging based on a lightweight request, response approach.

publications and other acoustic modems and localization algorithms.

II. Ranging

In the following section we present our approach for a time-of-flight based two-way ranging to measure distances between two μAUVs. We analyzed the performance of our approach and the influence of false speed-of-sound measurements.

A. Approach

For distance-based self-localization an accurate distance measurement between μAUVs is needed. The distance of μAUVs is commonly between 5 m to 100 m in the targeted use case; therefore, accuracy of the distance measurements should be in the range of a few centimeter. As described in Sect. I, communication, ranging and localization should be done by one single device in the μAUV to lower cost and complexity. Due to extremely low data rates of only a few hundred bit per second, distance measurements piggy-backed on standard communication packets are desired to save bandwidth.

Furthermore, we do not promote a solution that relies on time synchronization, because it adds additional (protocol) overhead and would require microsecond precision to achieve sub-meter ranging accuracy. Due to the relative low speed of sound for acoustic waves, underwater time-of-flight measuring gives a good precision w.r.t to the available time resolution, i.e. to achieve a precision of 1 cm a time resolution of 6.67 µs is needed, assuming a speed of sound of $1500\,\mathrm{m\,s^{-1}}$ (cf. Sect. II-B). Following all this, two-way time-of-flight ranging is the used approach for distance measurements. This can be achieved by almost any modem in the price and size range of the desired use case. If not already implemented, it can be added with little effort if the user has access to the modem firmware. If not, but the processing time of the modem is known and constant or can be estimated, then measuring distance via time-of-flight can also be achieved.

In the case of our self-developed modem—that we presented in [5]—two-way ranging is enabled by setting a flag in a transmitted packet, requesting a range measurement. As depicted in Fig. 1 the sender records the time $t_{q,tx}$ at the end of transmission. On reception of this packet, the receiver records its processing duration T_p of the packet

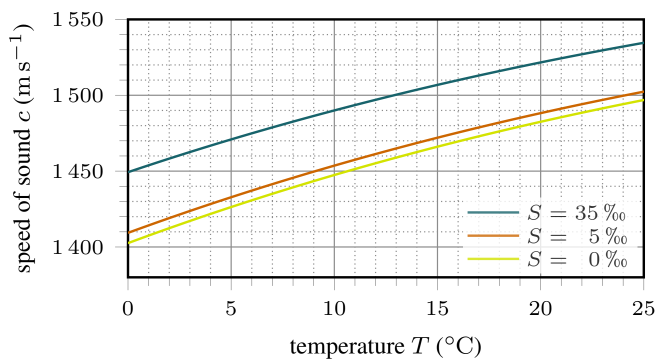

Fig. 2: Variation of the speed-of-sound underwater over temperature for fresh- (0 ‰), brackish- (5 ‰) and sea-water (35 ‰) at a depth of 10 m.

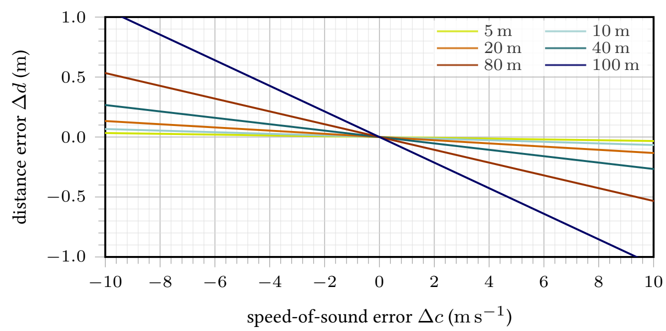

Fig. 3: Error of distance measurement induced from a false speed-of-sound estimation for distances up to 100 m.

and responds with an acknowledgment containing this duration. On reception of the response (acknowledgment) by the sender at time $t^*_{r,rx}$, the time-of-flight T_w in one direction can be calculated as

$$T_{\mathrm{w}} = \frac{t^*_{\mathrm{r,rx}} - t_{\mathrm{q,tx}} - T_{\mathrm{p}}}{2}. \tag{1}$$

By applying the speed of sound in water c (which can be pre-programmed at mission start or measured by the on-board-sensors) the distance to other μAUVs can be calculated as

$$d_{\mathrm{SR}} = c \cdot T_{\mathrm{w}}. \tag{2}$$

Details on the algorithm are presented in [6]. This approach assumes a nearly homogeneous water body w.r.t. speed of sound, which is true in many shallow-water applications as discussed below. A quick remedy for different values at sender and receiver (under the assumption of a linear gradient between them), is calculating the mean speed of sound at sender and receiver, which may yield a better approximation at short distances. This can be achieved by attaching the speed of sound at the receiver to the ranging response.

B. Speed of Sound

An important aspect of accurate time-of-flight based ranging measurements is an accurate knowledge of the speed of sound in water. The propagation speed of an acoustic signal underwater mainly depends on three parameters, namely depth, temperature and salinity.

A variety of publications exists, providing empirically determined, equations to estimate the speed of sound from these three parameters. Simple equations have been proposed by Mackenzie [7] and Coppens [8]. Refined equations, requiring a more complex calculation, are the UNESCO equation [9], [10], [11] or the Del Grosso's equation [12]. As it is the most commonly used equation, we will be using the UNESCO equation in the remainder of this paper.

We analyzed the influence of each of the three parameters. For the designated use cases, we expect temperatures in the range of 4 °C to 25 °C. The expected salinity ranges from 0 ppm to 35 ppm; however, we expect this to be nearly constant during each mission and therefore known. The missions and applications we envision for are commonly in shallow water and therefore depth is expected to be 0 m to 20 m. The results, depicted in Fig. 2, show that the speed of sound mainly depends on the water temperature. We assume that this can be measured from the μAUV, as temperature sensors are comparably cheap and easily integrable. Note, that many μAUVs are equipped with a depth sensor for position control, too.

Although we expect that the speed of sound can be measured with an error of less than $10\,\mathrm{m\,s^{-1}}$, we analyzed the deviation of our ranging results assuming a notably error-afflicted speed of sound. The results in Fig. 3 show the error of ranging due to imprecise speed-of-sound measurements. Assuming that depth and salinity are known and constant and that temperature can be measured with a precision of 1 °C, the error in speed-of-sound calculation is smaller than $10\,\mathrm{m\,s^{-1}}$ and the resulting ranging error is less than 1 m at a distance of 100 m. Thus, we expect the error of distance measurements due to wrong speed-of-sound estimation to be smaller than 1 %. The absolute error is small compared to the error induced by standard GNSS receivers.

A practical evaluation of the ranging method implemented at our self-developed modem is given in Sect. V.

III. Localization

This section presents a leightweight algorithm for self-localization of small, submerged μAUVs based on the availability of anchor μAUVs with a known position.

A. Prerequisites and Geometry

The general goal of self-localization is to determine the 3D-position of a μAUV in x, y, and z-direction. As μAUVs are usually equipped with a depth sensor, we can assume that the z-coordinate of each μAUV is known up to a precision of a few centimeters. We also assume that μAUVs are equipped with GNSS, e.g. GPS, so non-submerged μAUVs can determine their x and y position. For the discussed use cases, the μAUVs will be deployed in formations with distances of several meters, so GPS-accuracy is assumed to be sufficient. Positions of non-submerged nodes are used as reference for localization. In the following we assume every μAUV to be numbered by an ID $i \in \mathbb{N}(i < N, N \equiv \text{number of } \mu\text{AUVs})$. The position of a μAUV i is defined as $\boldsymbol{p}_\mathrm{i} = (x_\mathrm{i}, y_\mathrm{i}, z_\mathrm{i})$. W.l.o.g., the to-be-localized μAUV gets assigned ID 0, whilst the non-submerged μAUVs, in the following called anchors, are assigned in ascending order with $i = 1, 2, \ldots$. Following this, we can assume that $\boldsymbol{p}_\mathrm{i}$ is known for all $i \geq 1$, i.e. through GNSS. z_i is, however, known for every μAUV, we define the water surface as reference plane for z, hence it is 0 for all anchors, and measured through the depth sensor by the submerged μAUV. The distance between a μAUV i and j is denominated as $d_{i,j}$.

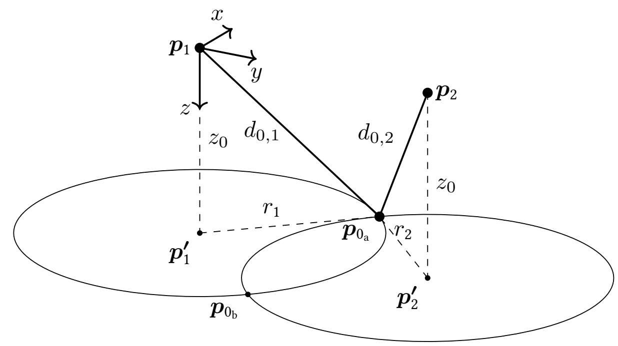

Fig. 4: Projection of $\boldsymbol{p}_1$ and $\boldsymbol{p}_2$ into the plane of $\boldsymbol{p}_0$. To determine $\boldsymbol{p}_0$, we use the measured distances $d_{0,n}$.

In the case of two available anchors, the situation is as shown in Eq. (3). Since z_0 is known, the positions $\boldsymbol{p}_1$ and $\boldsymbol{p}_2$ can be projected into the horizontal plane of $\boldsymbol{p}_0$, called $\boldsymbol{p}'_1$ and $\boldsymbol{p}'_2$. This gives two circles

$$r_\mathrm{i}^2 = (x_0 - x_\mathrm{i})^2 + (y_0 - y_\mathrm{i})^2 \qquad i \in \{1, 2\}. \tag{3}$$

Due to the projection into horizontal plane of $\boldsymbol{p}_0$ we obtain

$$r_\mathrm{i}^2 = d_{0,i}^2 - z_0^2 \qquad i \in \{1, 2\}. \tag{4}$$

The two circles have two intersections, representing the two possible locations $\boldsymbol{p}_{0_\mathrm{a}}$, $\boldsymbol{p}_{0_\mathrm{b}}$ of μAUV 0. Combining Eq. (3) and Eq. (4) for each i, and subtracting the results from each other yields

$$2x_0x_1 + 2y_0y_1 - x_1^2 - y_2^2 - r_1^2 + r_2^2 = 0. \tag{5}$$

This equation represents the line defined by the two intersection points. The problem is thus reduced to a line-circle intersection problem with two possible solutions where μAUV 0 could be located. Our algorithm, presented in the next section, will take care of this ambiguity.

If three anchors are available, we obtain another circle as depicted in Fig. 5. Equation (3) and Eq. (4) are modified

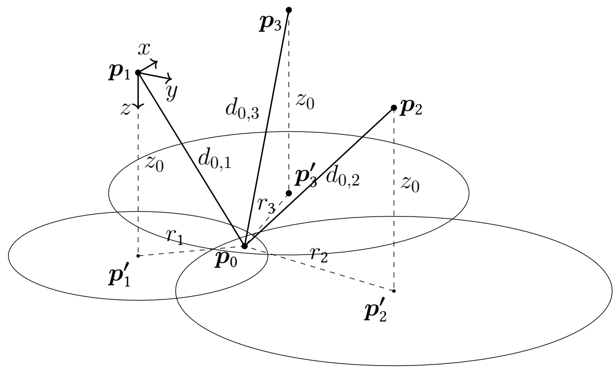

Fig. 5: Projection of $\boldsymbol{p}_1$, $\boldsymbol{p}_2$ and $\boldsymbol{p}_3$ into the plane of $\boldsymbol{p}_0$. To determine the solution for $\boldsymbol{p}_0$ we use the measured distances $d_{0,1}$, $d_{0,2}$ and $d_{0,3}$.

by an increased set $i \in \{1, 2, 3\}$. If a perfect speed-of-sound measurement, anchor positioning and ranging is assumed, this leads to a unique solution. As this is not the case in the real world, no exact solution exists. Instead an overlapping area may occur inside the node is located. Another possibility is, that no solution does exists. The localization algorithm has to determine a single solution for those cases, i.e. by using minimizing the mean square error.

B. Algorithm

The proposed localization algorithm is based on two-way ranging (cf. Sect. II) and the assumptions made in the previous section. At the beginning of each mission, all μAUVs are on the surface and know their position. After submersion, x_0 and y_0 become unknown and must therefore be determined by the localization process. The IDs of all available anchors are known by all participating μAUVs, and can be stored at mission start. The proposed algorithm works as follows: The node sends a packet to a broadcast address with the ranging-request flag set . After having overheard this request, the first anchor immediately answers with a response. The second anchor sends its own response after overhearing the one sent by the first anchor or after a timeout of $t_{\max}$ has been elapsed. The same holds for the third anchor. All the ranging responses contain the corresponding position of the anchor. After receiving all responses or after a timeout of $(n+1) \cdot t_{\max}$ has been elapsed a new round is started and another request can sent by the to-be-localized μAUV. The time $t_{\max}$ is determined by the speed of sound c, the length l of the packet, the data rate R of the used acoustic modem and the maximum distance between sender and receiver $d_{\max}$. It is calculated as

$$t_{\max} = \left(\frac{d_{\max}}{c} + \frac{l}{R} \right). \tag{6}$$

For our self-developed acoustic modem ($R = 266\,\mathrm{bit\,s^{-1}}$) and a packet length of 15 B (header and payload of two

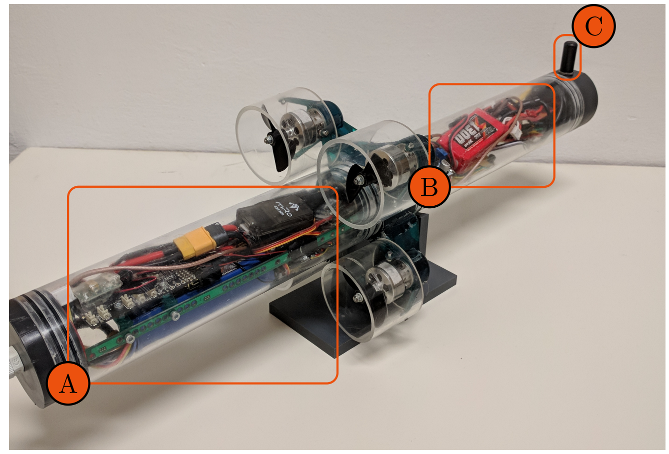

Fig. 6: HippoCampus Testbed with integrated A) pixhawk controller, main battery and telemetry transmitter; B) acoustic modem and Raspberry Pi with own battery and C) hydrophone mounted to the hull of the μAUV. The external WiFi antenna is not included in the picture, the external connection to it, is shown on the very left end of the μAUV.

sensor values), a maximum expected distance of 150 m, and a minimal speed of sound of $1400\,\mathrm{m\,s^{-1}}$ a value of 1.06 s was calculated for $t_{\max}$.

The behavior of the localization algorithm after each round depends on the number of received ranging responses. If less than two responses are received, no localization is done. If exactly two responses are received two exact solutions are calculated as described in the beginning of this section. The node choses the solution as new estimated position which has a smaller euclidean distance to the last known position. Due to distances between μAUVs of several meters and a comparable slow movement of a few meters per second this is a feasible approach. If more than two responses are received, there is not necessarily an exact solution due to distance measurement errors. We use a least square estimation to determine the position minimizing the distance error to all circles found by the two-way ranging and the projection into the plane.

IV. Hardware Integration

For practical evaluation of the feasibility of self-localization of μAUVs with small and low-cost acoustic modems a testing platform is needed, with a) an integrated low-cost acoustic modem allowing time-of-flight ranging, b) a fixed depth, so that measurements are not influenced by varying distances induced by changed depth, c) the ability of sailing the test platform by hand, so that desired trajectories can be sailed and d) the availability of reference positions to compare against.

For communication, we use our small, self-developed, low-cost acoustic underwater modem, due to its low-cost and availability at the institute. The communication distance of our modem is at least 150 m with a

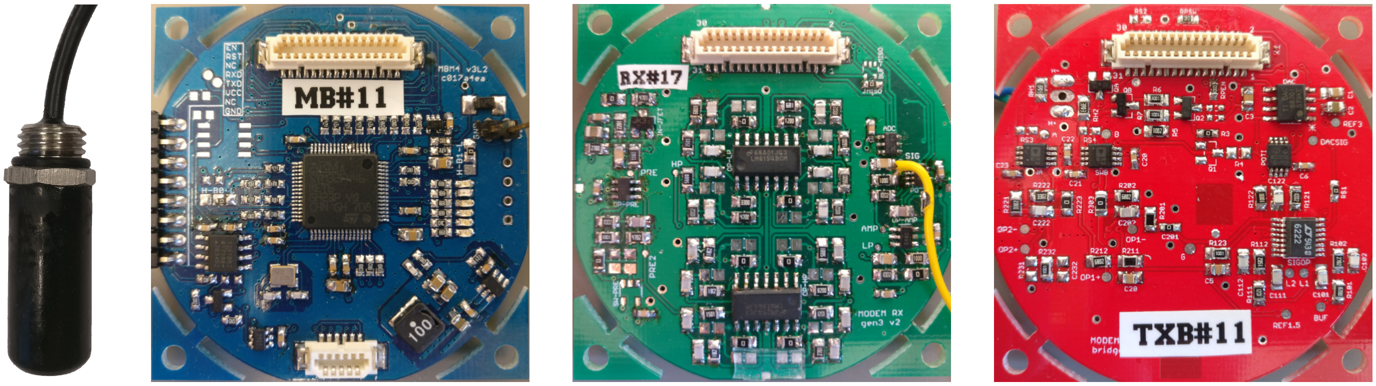

Fig. 7: Acoustic modem prototype (left to right): hydrophone, mainboard (blue), receive filter and amplifier (green), bridge send power amplifier (red). Note that the power amplifier has half of its components on the back side. All components are shown in actual size without scaling.

data rate of up to 4.7 kbit s^{-1}. With a price of only €600 including hydrophone and form factor of only 50 mm × 50 mm × 25 mm (see Fig. 7) it is designed for the use in small and low-cost μAUVs. A detailed presentation of our modem is given in [5]. Note that the presented localization technique can be done with any other modem, if it provides time-of-flight measuring or any other kind of ranging.

We integrated our modem in the HippoCampus [4] μAUV. We chose the HippoCampus as it perfectly fits our targeted use case of low-cost, small μAUVs. The HippoCampus can be easily extended by additional hardware and is available at the TUHH. The movement of the robot is controlled via a pixhawk [13] control board. As an autonomous behavior is not needed or desired during our evaluation, we control the robot with an off-the-shelf RC radio control transmitting on the 40 MHz-band. The telemetry data of the robot is sent out from the pixhawk board via a serial communication interface, connected to a 433 MHz serial bridge. The data can be observed during the tests via the QGroundcontrol software, commonly used for multicopters. Of course, the range of this connection is strictly limited to a few meters; however, telemetry is not needed during the evaluation. For later uses cases it is planned to send telemetry data over the acoustic link.

To have a fair comparison between different evaluations, depth and orientation of the robot should be fixed. Therefore, we attached a threaded rod to the chassis of the robot, as shown in Fig. 6. At the other end of the rod we mounted a cross out of aluminum profiles with a diameter of 100 cm. Blocks of polystyrene were mounted to every end to the cross ensuring a fixed depth and a stable position of the submerged robot.

For simplicity and easy live-tracking of the evaluation process we integrated a Raspberry Pi Zero W into the robot. An external WiFi antenna was attached to the Raspberry Pi. The antenna itself is fixed at the top of the aluminum cross to ensure continuous connection between the Raspberry Pi and the WiFi used by the rest of our evaluation equipment. The acoustic modem is finally connected to the Raspberry Pi via a serial connection. The hydrophone used for transmission and reception of the packets is directly mounted to the hull of the robot with a thread. To be able to compare our localization results against a ground truth, we connect a Navilock NL-8001U GNSS receiver to another Raspberry Pi at the water surface.

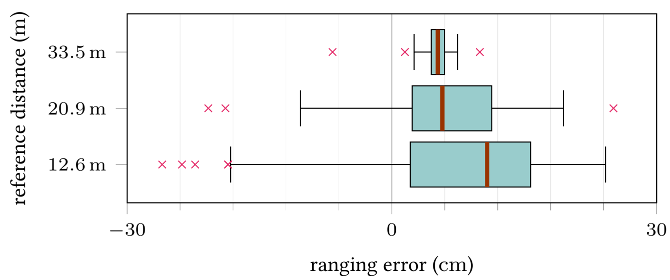

Fig. 8: Results of two-way time-of-flight ranging for several distances of modems deployed at a jetty in Hamburg-Harburg.

V. Practical Evaluation

In the following section we describe our experiences and results during the evaluation of our time-of-flight based ranging, our localization for the static and mobile case. In all cases we determined the speed of sound with a professional CTD-48[1] probe, manufactured by Sea&Sun Technologies, allowing a precise speed-of-sound measurement. For all evaluated cases the hydrophone were placed in the same depth of around 90 cm.

A. Ranging

For evaluation of the proposed two-way time-of-flight ranging we deployed multiple acoustic modems at a jetty

[1]http://www.sea-sun-tech.com/marine-tech/hydrology/ctd-multiparameter-probe/ctd-48-multiparameter-probe.html

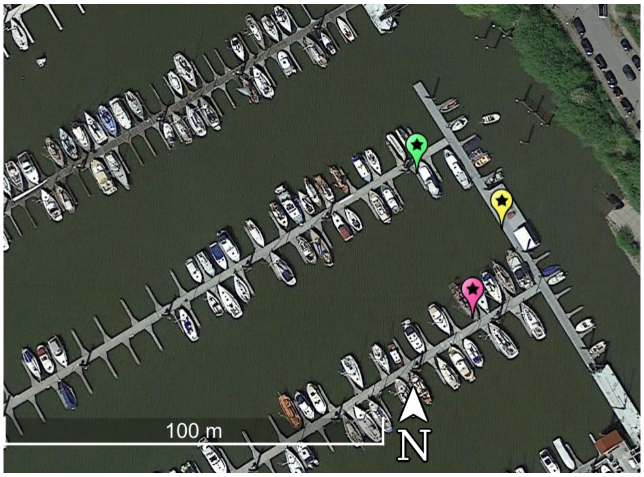

Fig. 9: Test setup for evaluation of static localization in Hamburg-Finkenwerder. During tests no boats were in the water. Image © Google Earth.

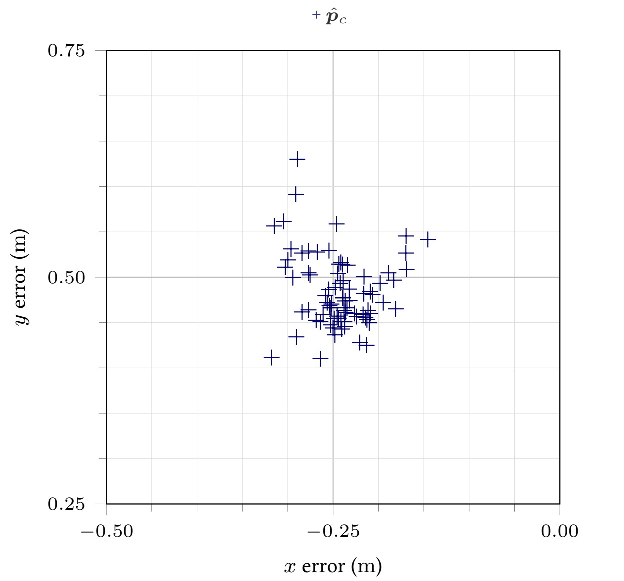

Fig. 10: Localization error during outdoor experiment with anchors at $(25.4\,\mathrm{m}, 19.3\,\mathrm{m})$, $(-17.4\,\mathrm{m}, 20.8\,\mathrm{m})$ and node at $(0\,\mathrm{m}, 0\,\mathrm{m})$ in Hamburg-Finkenwerder. $\hat{\boldsymbol{p}}_c$ denotes the estimated positions.

at the Harburg Channel. To obtain an accurate ground truth we used a Leica Disto A5 [14], a laser distance measuring tool, providing a reference distance with an accuracy of at least 1 cm. For each pair of the three deployed modes 100 ranging requests were sent. We received 94 responses for the distance of 12.6 m, 90 for 20.9 m and 100 for 33.5 m. The standard deviation was 11.8 cm, 9.3 cm and 1.7 cm respectively, as shown in Fig. 8. In total we were able to achieve a reliable distance measurement with an error of less than 30 cm. With a sampling time of 5 µs and a speed of sound of $1500\,\mathrm{m\,s^{-1}}$ the minimal achievable accuracy is 7.5 mm. The error of our distance measurements is mainly caused by reflections at the water surface, small hydrophone movements due to water current and inaccurate packet-based synchronization. At larger distances the difference between line-of-sight distance and the distance via the water surface becomes smaller. We therefore expect the error to be smaller at larger distances and were able to confirm that by our measurements. We also did measurements for 90 m and 150 m, omitted in Fig. 8 due to no additional insight. These measurement basically show the same precision.

B. Localization - Static Case

To test our algorithm in the static case, we deployed three modems at jetties in a marina in Hamburg-Finkenwerder. Three hydrophones were placed in a triangular shape with a distance of several meters. We sent 100 ranging requests each, one every 2 s. The setup is shown in Fig. 9. From 100 ranging requests both answers were received in 79 % of the cases. Localization was only done if both answers were received, runs in which only one answer (19 %) or even none (2 %) was received were skipped. To obtain a ground truth, we measured the distances of the hydrophones with a tapeline on the jetties. The results of self-localization, shown in Fig. 10, reveal that we are able to obtain a very precise position with a standard deviation of 3.54 cm in x-direction and 3.97 cm in y-direction. The mean error of our obtained ground truth was 24.25 cm in x-direction and 48.42 cm in y-direction. This leads to a mean euclidean distance error of 54.15 cm, resulting from acoustic reflections at the water surface and from a possibly inaccurate ground truth (jetties not orthogonal, hydrophone moved by currents).

C. Localization - Mobile Case

Finally, we evaluated our localization approach in a mobile case. We deployed three anchor modems as depicted in Fig. 11. The distances between these modems are the same as given in Sect. V-A. We placed the HippoCampus equipped with our test equipment as described in Sect. IV in the water and sailed a trajectory roughly rectangular with a side length of approximately $10\,\mathrm{m} \times 30\,\mathrm{m}$. During the sailing of the desired trajectory the robot sent a ranging request every 3 seconds and the localization algorithm was implemented as described in Sect. III. In total, 100 requests have been sent and 86 responses have been received from the anchor in the middle, 36 from the right and 41 from the left anchor. Compared to our findings during the evaluation of the ranging the packet reception rates are comparably low, except for anchor placed in the middle. We expect this resulting from the placement of the hydrophone at the μAUV and the water current on the hydrophones during sailing. As we were still able to gather enough data for a self-localization, resolving this issue is not done during this paper, but still on our agenda.

Fig. 11: Testsetup at the Harburg Channel, anchors estimated with laser distance measurement and Google Earth. The anchors were deployed on a jettie, not included in the satellite image. The recorded GPS track of the μAUV is also shown. As the robot was only sailing eastern of the jetty (and the anchors), a false GPS measurement is clearly visible. Image © Google Earth.

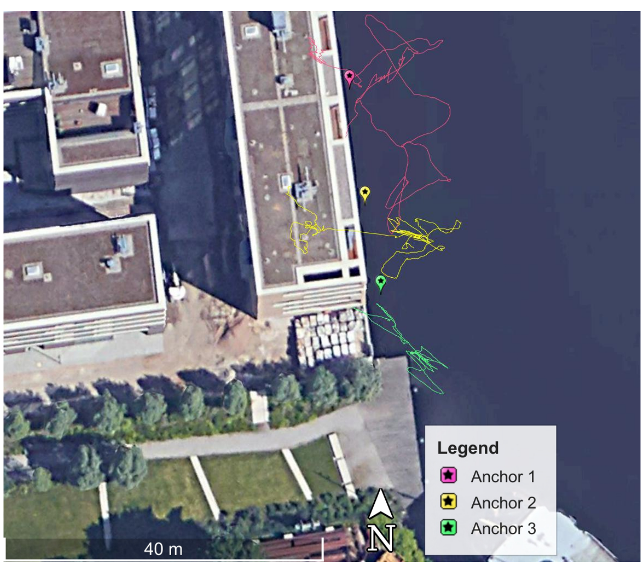

Fig. 12: Testsetup at the Harburg Channel, with GPS estimated anchors. Obviously using the GPS measured anchors as a reference for precise self-localization will not give usable results. Image © Google Earth.

The route, resulting from the localization process, is shown in Fig. 14. Due to the geometry of the jetty the anchors were on a straight line, so we assumed that line to be the y-axis of our cartesian coordinate system, so that $x_i = 0 | i \in \{1, 2, 3\}$ holds.

The sailed trajectory fits to the desired trajectory but is off a few meters. To have a ground truth comparison in addition to our visual inspection of the sailed course, we compared the logged GPS route of the μAUV to the route calculated by the localization algorithm. For that, the exact GPS position of the anchor modems has to be known. We tried to average the position of each of those modems. Unfortunately, the accuracy of the GPS receiver available to us, is, in combination with the near wall of a house, resulting in poor reception, not good enough to calculate a precise position. The logged track for each of the anchors is depicted in Fig. 11. As each of those tracks fluctuates by up to 30 m the gained GPS position is not usable for evaluation of our localization algorithm.

However, to evaluate our results against any kind of ground truth a correlation of logged GPS track and calculated track is needed. Following this we stick to the already known cartesian coordinate system. The GPS track of the robot thus has to be converted from latitude/longitude to x/y-coordinates. We used AlvinXY projection for that, developed in 1960's, an implementation described in [15]. As our assumption that the anchors lay completely horizontal on the y-axis does not hold in this case, we measured the angle α the cartesian coordinate system had to be turned to fit the GPS coordinates via the Google Maps tool and simple trigonometry and calculated a value of $\alpha = 6.38\,\text{deg}$. Thus, all latitude/longitude points of the logged GPS track were converted via AlvinXY projection and then rotated via the rotation matrix

$$R_\alpha = \begin{pmatrix} \cos\alpha & -\sin\alpha \\ \sin\alpha & \cos\alpha \end{pmatrix}. \tag{7}$$

The result, calculated path vs. logged track are depicted in Fig. 15. The calculated positions clearly fit the logged track, however while the μAUV is near to the building (cf. Fig. 11) the GPS track has a remarkable offset. This offset is even visible when we compare the GPS track to a satellite image, depicted in Fig. 12 and showing the belief of GPS, that the robot is sailing on the land.

D. Lessons Learned

During our practical evaluation of ranging and localization we faced a few challenges. The main and most important one is the determination of an accurate ground truth for mobile localization. As our ranging measurement have an error of less than 30 cm we expect our localization to be precise in the same order of magnitude. We were able to show that for the static case. However, for the mobile case there is no (inexpensive) ground truth available with a precision better we our localization approach to be. On the contrary, GPS induces an error of at least 2 m in the

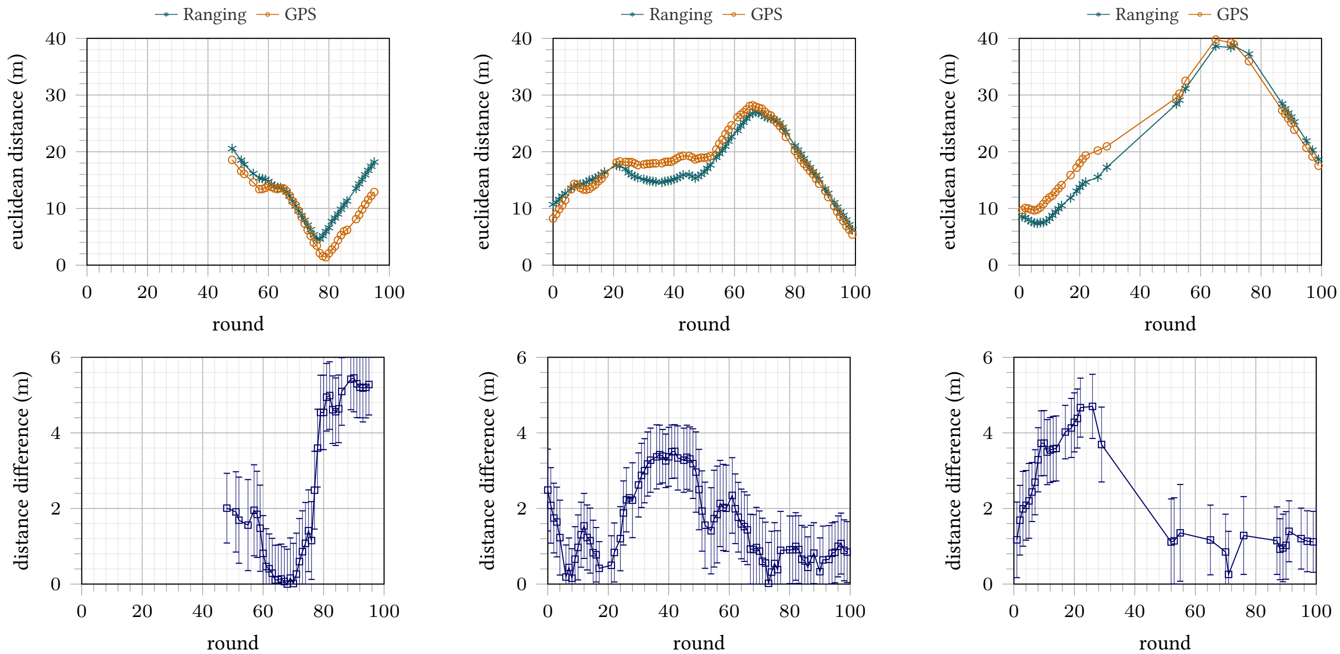

Anchor 1 vs. GPS

Anchor 2 vs. GPS

Anchor 3 vs. GPS

Fig. 13: Acoustic distance measurements from the μAUV to each anchor, compared to the measured GPS distance. The error bars in the bottom row indicate the GPS error, provided by the GPS receiver.

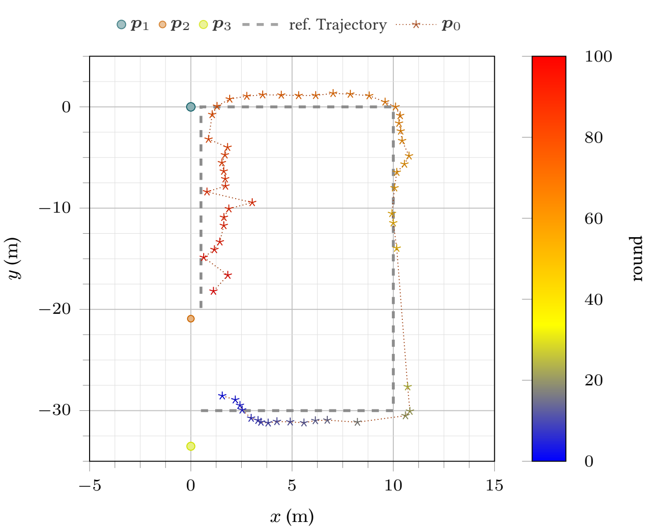

Fig. 14: Estimated path determined by the localization algorithm compared to desired sailed trajectory.

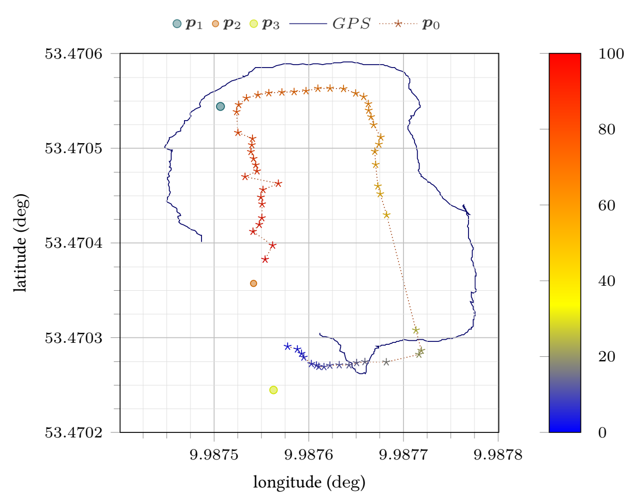

Fig. 15: Self-localized position compared to logged GPS positions.

best case; however, during our evaluation we experienced an error way higher. Following this, the assumption made by many μAUV developing researchers, that the position of a μAUV equipped with a simple GNSS receiver can be assumed to be known is at least questionable.

Another aspect is the difficulty to sail a specific trajectory with a hand controlled robot. Without any kind of mechanical guidance a straight line can only roughly be followed. However, this is not practicable for the distance we aim for.

Due to the delay between reception of multiple ranging responses our approach is only applicable for μAUVs with a small speed at the moment. The application for faster μAUVs has still to be investigated.

VI. Related Work

Various communication devices for underwater applications exist, developed by academia and industry. The

WHOI Micro-Modem [16], [17] is one of the most common proposals from academia, yet with a price of several thousand dollars and therefore exceeding the cost of the μAUV (price of Hippocampus is around \$ 600) it is inapplicable. This also holds for the modems manufactured by Evologics [18] and Teledyne [19]. Other modems, like the one presented by Nowsheen et. al [20] or Cario et. al [21] are based on an FPGA or DSP and hamper fast and easy development of novel algorithms, as knowledge on microcontrollers is more common for researchers in the computer science field. Despite from this fact the usage of modems in this price class for the presented localization algorithm is conceivable.

Furthermore, several underwater localization algorithms have been presented by the research community in the recent years, as shown in [22], [23]. Centralized algorithms, like ALS [24] are not applicable for self-localization of swarm members. Algorithms requiring stationary anchors, like UPS [25] are not suitable for the designated use case too, as they hamper the flexibility of deployment of swarms without existing infrastructure. Algorithms relying on synchronized nodes (HASL [26]) or using multiple receivers for angle of arrival estimation are raising cost and complexity and are therefore not appropriate. This holds for all techniques introducing additional hardware like sonar or DVL. In addition to acoustic localization, a few localization algorithm based on radio signals, like [27] or on optical communication as presented in [28] are not applicable due to their low range and robustness in murky water.

VII. Conclusion and Outlook

We showed that self-localization of μAUVs is generally feasible by only using simple time-of-flight ranging, a technique that is, amongst others, provided by our self-developed acoustic modem. We described lightweight algorithms for two-way ranging and self-localization. We described the building of a low-cost evaluation platform based on the HippoCampus and an acoustic modem. During practical evaluations we analyzed the single compartments (ranging, static and mobile localization) for their reliability and performance. We noticed that nothing more than the proposed hardware and algorithm is needed for self-localization. Our evaluation were realistic for the desired use case of environmental monitoring in swarm, as we used an already existing μAUV in a fixed depth, simulating the inspection of a certain depth.

However, we also noticed that obtaining an accurate ground truth is essential for our simple localization algorithm and hard to obtain in practice without buying costly hardware. In the future we will further improve our localization algorithm, making it more robust against missing ranging responses. In addition to that we will also look at obtaining a more precise anchor ground truth, e.g. by using free real-time kinematic service for GNSS or implementing dead reckoning during short periods between localization results. Also on the agenda is the consideration of previously calculated positions to improve the position estimation.

Acknowledgement

This work has been partially supported by the German Federal Ministry of Education of Research (BMBF) under grant number 13N14153. The authors would like to thank Thies Oelerich for his assistance with building the evaluation platform and the Institute of Mechanics and Ocean Engineering, especially Daniel Dücker, for providing the HippoCampus vehicle.

References

[1] B. Meyer, C. Isokeit, E. Maehle, and B. Baschek, “Using Small Swarm-Capable AUVs for Submesoscale Eddy Measurements in the Baltic Sea,” in Proceedings of the MTS/IEEE Oceans Conference, OCEANS, Sept. 2017.

[2] C. Osterloh, B. Meyer, A. Amory, T. Pionteck, and E. Maehle, “MONSUN II – Towards Autonomous Underwater Swarms for Environmental Monitoring,” in Proceedings of the IROS2012 Workshop on Robotics for Environmental Monitoring, Oct. 2012.

[3] B. Meyer, K. Ehlers, C. Isokeit, and E. Maehle, “The Development of The Modular Hard- and Software Architecture of the Autonomous Underwater Vehicle MONSUN,” in ISR/Robotik 2014; 41st International Symposium on Robotics, pp. 1–6, June 2014.

[4] A. Hackbarth, E. Kreuzer, and E. Solowjow, “HippoCampus: A Micro Underwater Vehicle for Swarm Applications,” in Proceedings of the IEEE/RSJ International Conference on Intelligent Robots and Systems, IROS, (Hamburg, Germany), 2015.

[5] C. Renner and A. J. Golkowski, “Acoustic Modem for Micro AUVs: Design and Practical Evaluation,” in ACM WUWNet, 2016.

[6] C. Renner, “Packet-Based Ranging with a Low-Power, Low-Cost Acoustic Modem for Micro AUVs,” in SCC 2017; 11th International ITG Conference on Systems, Communications and Coding, pp. 1–6, Feb 2017.

[7] K. V. Mackenzie, “Nine-term equation for sound speed in the oceans,” The Journal of the Acoustical Society of America, vol. 70, no. 3, pp. 807–812, 1981.

[8] A. B. Coppens, “Simple equations for the speed of sound in neptunian waters,” The Journal of the Acoustical Society of America, vol. 69, no. 3, pp. 862–863, 1981.

[9] C. Chen and F. J. Millero, “Speed of sound in seawater at high pressures,” The Journal of the Acoustical Society of America, vol. 62, no. 5, pp. 1129–1135, 1977.

[10] N. P. Fofonoff and R. Millard, “Algorithms for Computation of Fundamental Properties of Seawater,” vol. 44, 01 1983.

[11] G. S. K. Wong and S. Zhu, “Speed of sound in seawater as a function of salinity, temperature, and pressure,” The Journal of the Acoustical Society of America, vol. 97, no. 3, pp. 1732–1736, 1995.

[12] V. A. Del Grosso, “New equation for the speed of sound in natural waters (with comparisons to other equations),” The Journal of the Acoustical Society of America, vol. 56, no. 4, pp. 1084–1091, 1974.

[13] Pixhawk, “Product Page Overview.” https://pixhawk.org/#autopilots. Accessed: 2018/07/26.

[14] Leica Geosystems, “Leica DISTO A5 The Original Laser Distance Meter.” https://ptd.leica-geosystems.com/downloads123/cp/general/a5/manuals/LeicaDISTO_A5_de.pdf. Accessed: 2018/07/26.

[15] C. Murphy and H. Singh, “Rectilinear coordinate frames for deep sea navigation,” in 2010 IEEE/OES Autonomous Underwater Vehicles, pp. 1–10, Sept 2010.

[16] L. Freitag, M. Grund, S. Singh, J. Partan, P. Koski, and K. Ball, “The WHOI Micro-Modem: An Acoustic Communications and Navigation System for Multiple Platforms,” in Proceedings of OCEANS 2005 MTS/IEEE, pp. 1086–1092 Vol. 2, Sept 2005.

[17] E. Gallimore, J. Partan, I. Vaughn, S. Singh, J. Shusta, and L. Freitag, “The WHOI Micromodem-2: A Scalable System for Acoustic Communications and Networking,” in OCEANS 2010 MTS/IEEE SEATTLE, pp. 1–7, Sept 2010.

[18] Evologics GmbH, “Underwater Acoustic Modems Product Information.” https://www.evologics.de/en/products/acoustics/index.html. Accessed: 2018/07/26.

[19] Teledyne Marine, “Underwater Acoustic modems for Wireless Communication.” http://www.teledynemarine.com/acoustic-modems. Accessed: 2018/07/26.

[20] N. Nowsheen, C. Benson, and M. Frater, “A High Data-Rate, Software-Defined Underwater Acoustic Modem,” in In Proceedings of the MTS/IEEE Oceans Conference, OCEANS, (Sydney, Australia), May 2010.

[21] G. Cario, A. Casavola, M. Lupia, and C. Rosace, “SeaModem: a Low-Cost Underwater Acoustic Modem for Shallow Water Communication,” in OCEANS 2015 - Genova, pp. 1–6, May 2015.

[22] H.-P. Tan, R. Diamant, W. K. Seah, and M. Waldmeyer, “A Survey of Techniques and Challenges in Underwater Localization,” Ocean Engineering, vol. 38, no. 14, 2011.

[23] M. Erol-Kantarci, H. T. Mouftah, and S. Oktug, “A Survey of Architectures and Localization Techniques for Underwater Acoustic Sensor Networks,” IEEE Communications Surveys & Tutorials, vol. 13, pp. 487–502, Sept. 2011.

[24] V. Chandrasekhar and W. Seah, “An Area Localization Scheme for Underwater Sensor Networks,” in OCEANS 2006 - Asia Pacific, pp. 1–8, May 2006.

[25] X. Cheng, H. Shu, Q. Liang, and D. Du, “Silent Positioning in Underwater Acoustic Sensor Networks,” IEEE TVT, vol. 57, no. 3, 2008.

[26] T. Bian, R. Venkatesan, and C. Li, “Design and Evaluation of a New Localization Scheme for Underwater Acoustic Sensor Networks,” in GLOBECOM 2009 - 2009 IEEE Global Telecommunications Conference, pp. 1–5, Nov 2009.

[27] A. D. Buchan, E. Solowjow, D. A. Duecker, and E. Kreuzer, “Low-cost Monocular Localization with Active Markers for Micro Autonomous Underwater Vehicles,” in 2017 IEEE/RSJ International Conference on Intelligent Robots and Systems (IROS), pp. 4181–4188, Sept 2017.

[28] M. Pelka, M. Mackenberg, C. Funda, and H. Hellbrück, “Optical Underwater Distance Estimation,” in OCEANS 2017 - Aberdeen, pp. 1–6, June 2017.